



OPEN

Fixed-target protein serial microcrystallography with an x-ray free electron laser

SUBJECT AREAS:

NANOCRYSTALLOGRAPHY
STRUCTURE DETERMINATIONReceived
14 May 2014Accepted
4 July 2014Published
12 August 2014Correspondence and
requests for materials
should be addressed to
M.F. (frank1@llnl.gov)

Mark S. Hunter¹, Brent Segelke², Marc Messerschmidt³, Garth J. Williams³, Nadia A. Zatsepin⁴, Anton Barty⁵, W. Henry Benner², David B. Carlson⁶, Matthew Coleman^{2,7}, Alexander Graf¹, Stefan P. Hau-Riege¹, Tommaso Pardini¹, M. Marvin Seibert³, James Evans^{6,8}, Sébastien Boutet³ & Matthias Frank¹

¹Physics Division, Lawrence Livermore National Laboratory, 7000 East Avenue, Mail Stop L-211, Livermore, CA 94550, USA, ²Biosciences and Biotechnology Division, Lawrence Livermore National Laboratory, 7000 East Avenue, Mail Stop L-452, Livermore, CA 94550, USA, ³Linac Coherent Light Source, SLAC National Accelerator Laboratory, 2575 Sand Hill Road, Menlo Park, California 94025, USA, ⁴Department of Physics, Arizona State University, Tempe, AZ 85287, USA, ⁵Centre for Free-Electron Laser Science, DESY, Notkestrasse 85, 22607 Hamburg, Germany, ⁶Dept. of Molecular and Cellular Biology, University of California, Davis, 1 Shields Ave, Davis, CA, 95616, USA, ⁷Department of Radiation Oncology, University of California at Davis Medical Center, Sacramento, CA 95817, ⁸Environmental Molecular Sciences Laboratory, Pacific Northwest National Laboratory, 3335 Innovation Blvd., Richland, WA, 99354, USA.

We present results from experiments at the Linac Coherent Light Source (LCLS) demonstrating that serial femtosecond crystallography (SFX) can be performed to high resolution (~ 2.5 Å) using protein microcrystals deposited on an ultra-thin silicon nitride membrane and embedded in a preservation medium at room temperature. Data can be acquired at a high acquisition rate using x-ray free electron laser sources to overcome radiation damage, while sample consumption is dramatically reduced compared to flowing jet methods. We achieved a peak data acquisition rate of 10 Hz with a hit rate of $\sim 38\%$, indicating that a complete data set could be acquired in about one 12-hour LCLS shift using the setup described here, or in even less time using hardware optimized for fixed target SFX. This demonstration opens the door to ultra low sample consumption SFX using the technique of diffraction-before-destruction on proteins that exist in only small quantities and/or do not produce the copious quantities of microcrystals required for flowing jet methods.

X-ray crystallography has been the workhorse method for determining the high-resolution structures of proteins and protein complexes. However, conventional protein crystallography requires large (1000s of μm^3), well-ordered protein crystals and often requires measurements at cryogenic temperatures to mitigate radiation damage. The advent of x-ray free-electron lasers (XFELs), such as the Linac Coherent Light Source (LCLS)^{1,2} overcomes the need for large crystals and cryogenic temperatures. XFELs produce ultra-short (~ 10 – 50 fs) and ultra-bright x-ray pulses, enabling the collection of high-resolution diffraction patterns from protein crystals before the onset of conventional radiation damage (“diffraction-before-destruction”). Diffraction-before-destruction has been demonstrated with microcrystals that are too small to be considered for structure determination with conventional crystallography^{3,4}. Each microcrystal exposed to an XFEL pulse is destroyed, necessitating a serial data acquisition approach in which a data set is collected from thousands of randomly oriented crystals, each exposed only once to the x-ray beam. First demonstrated using micrometer-sized crystals of the membrane protein photosystem I (PSI)³, serial femtosecond x-ray crystallography (SFX) has been extended to demonstrate high resolution structure determination⁵, has been used to observe novel high-resolution structural information⁶, and has been applied to solving the structure of a G-Protein Coupled Receptor (GPCR) embedded in lipidic cubic phase (LCP)⁷. For a recent review the use of x-ray lasers for structural and dynamic biology see⁸.

One of the drawbacks of the serial crystallography approach to date has been sample consumption, limiting the technique to samples that can be produced in large quantity. SFX experiments to date have used various forms of liquid jet injection, and the most often used injector is a gas dynamic virtual nozzle^{9–11}. The flow rate needed to

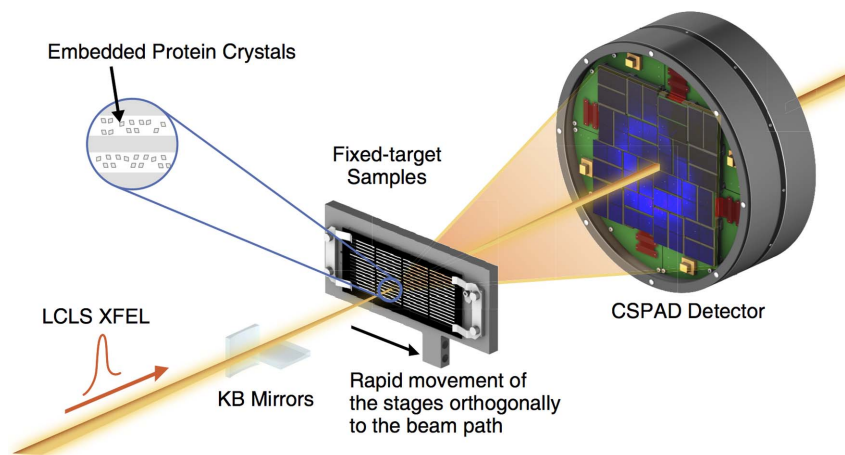


Figure 1 | Experimental overview. Protein crystals embedded in Paratone-N were placed on fixed-targets and measured *in vacuo* at the Coherent X-ray Imaging (CXI) beam line of the LCLS.

maintain the thin jet results in high linear velocity of liquid. As a result, only a very small fraction of the injected protein crystal suspension is probed by x-rays. An approach to SFX that reduces sample consumption is highly desirable, and may be essential for proteins that cannot be successfully over-expressed in large quantities. Slow flowing viscous jets extruded using electrospinning¹², direct injection of Lipidic Cubic Phase buffer^{7,13}, and pulsed injection provide alternatives in some cases. Yet another approach is to deposit sample on a thin membrane that is then scanned through the x-ray beam. Such a fixed-target approach allows for precise control of where the sample is measured with the x-rays resulting in a much more conservative use of the sample. The main limitation to date for fixed target approaches has been the relatively low data acquisition rate achieved so far: To date, SFX data sets require $\sim 10^4$ good diffraction patterns for reconstruction, each collected from randomly oriented crystals^{14,15}. Consequently, the data collection rate is a critical parameter.

Here, we demonstrate the first proof-of-principle results from fixed-target serial crystallography using the LCLS. Using microcrystals of REP24 (Rapid encystment protein, 24 kDa; pdb¹⁶ code 4P5P), a putative virulence factor protein from the intracellular pathogen *Francisella tularensis*, we demonstrate the ability to collect data at repetition rates that allow, in principle, for collection of complete data on the time scale of about one 12-hour LCLS shift.

Methods

Production of protein crystals. In order to produce microcrystals of REP24, several sparse-matrix crystallization screens were generated and used to make vapor-diffusion crystallization experiments using the sitting-drop technique. The sitting-drop experiments were carried out by mixing 400-nL aliquots of a 14.4 mg/mL REP24 solution (in 50 mM NaCl and 10 mM HEPES pH 7.5) with 400-nL aliquots of the precipitant solution at room temperature. The results of several screens were examined and optimization screens for sitting-drop crystallization experiments were generated around a condition that produced well-formed macrocrystals of REP24-containing 24% polyethyleneglycol-monomethylether with average molecular weight of 750 Da (PEG-MME 750) and 100 mM Na-Acetate, pH 4.5.

The results of the optimization screen were used to generate batch crystallization experiments for the production of the REP24 crystals in bulk. REP24 crystals were grown by mixing a 14.4 mg/mL REP24 sample (in 50 mM NaCl and 10 mM HEPES pH 7.5) with a precipitation solution containing 54% (v/v) PEG-MME 750 and 100 mM Na-acetate pH 4.5 in a 1:1 ratio for final conditions of 7.2 mg/mL REP24, 27% (v/v) PEG-MME 750, 50 mM Na-acetate pH 4.5, 25 mM NaCl, and 5 mM HEPES pH 7.5). The crystals of REP24 used in the experiment were between 10 μ m and 12 μ m in length and had the appearance of two, square-based pyramids connected at the peak, with maximum thickness of 5 μ m. In order to produce the REP24 microcrystals for the experiment, 190 μ L of the 14.4 mg/mL REP24 solution was used for a total protein mass of 2.74 mg. Approximately 1/5 of the protein could be used to cover an entire chip, for a total protein mass of 540 μ g of protein per chip.

Oil-emulsion preservation of protein crystals. Although moving protein macrocrystals from an aqueous environment to Paratone-N is well established, embedding a shower of microcrystals in Paratone-N and removing the aqueous phase

required a novel procedure. The REP24 crystal suspension in the mother liquor was filtered through a 20 μ m inline filter. The pre-filtered REP24 crystal suspension was centrifuged at $\sim 14,500$ g for one minute to generate a pellet. The supernatant was removed and the sample was again centrifuged at 14,500 g for one minute and the remaining supernatant was removed. An aliquot of 30 mg of Paratone-N was added to the pellet (to achieve approximately 50% hit rate), and a small pipette tip followed by a microspear were used to thoroughly mix the sample and suspend the crystals at a crystal density $\sim 1 \times 10^9$ crystals/mL.

Vigorous mixing with the microspear allowed for the protein crystals to be separated from the remaining bulk aqueous phase and into the Paratone-N, although crystals often remained surrounded by a small volume of aqueous mother liquor. The REP24 crystal emulsion was allowed to stand at room temperature for several days without a discernable decrease in birefringence of the REP24 microcrystals—further evidence that the crystals had not dehydrated.

Fixed target design and application of the sample to the fixed targets. Fixed-target supports allowed for high data-collection rates using the setup at the Coherent X-ray Imaging (CXI) beam line¹⁷ of the Linac Coherent Light Source (LCLS) at SLAC National Accelerator Laboratory. The fixed-target supports were silicon wafers produced by Silson Ltd (Silson Ltd, JBJ Business Park, Northampton Road, Blisworth, Northampton, NN7 3DW, England) and an individual wafer is shown in Fig. S1. The wafers were comprised of 200 μ m thick silicon crystals with a 50 nm Si₃N₄ layer deposited on the (100) face. Long, rectangular windows measuring 200 μ m \times 8400 μ m were etched into the silicon (leaving a 50 nm Si₃N₄ membrane) to allow for scanning of the sample through the LCLS x-ray beam through the use of the fixed-target stage motors. An overview of the experimental setup is shown in Fig. 1.

The sample was applied to the fixed-target wafers by covering the tip of a crystal-manipulation spear with a small drop of the crystal-containing emulsion. The drop was lightly touched to the windows on the Si₃N₄ side of the chip and gently “painted” across the long edge of the window, leaving a thick streak of the sample. A 1 mm diameter crystal-mounting loop was used to gently spread out the streak of sample between three rows of windows typically resulting in a sample thickness around 20 μ m. Once placed in the vacuum, the REP24 crystals embedded in Paratone-N were measured within 1–6 hours.

Experimental setup. REP24 samples were measured using the CXI instrument¹⁷ at LCLS using the (1.3 μ m)² focus sample environment. Fig. 1 shows a schematic overview of the experiment. The experiments were carried out using 8 keV x-rays (corresponding to a wavelength of 1.55Å) with an x-ray flux of $\sim 2 \times 10^{12}$ photons/pulse before accounting for losses due to upstream optics ($\sim 50\%$ loss) both at CXI and in the upstream shared part of the LCLS beam line; however, the x rays were attenuated such that transmission was between 0.1% and 10% during these experiments. Accounting for losses due to the upstream optics, the flux on the sample was between 1×10^9 – 1×10^{11} photons/pulse for the 0.1% and 10% transmission, respectively. The pulse durations used for the experiments were estimated to be ~ 30 fs based on recent measurements using the XTCAV diagnostics¹⁸.

Results

High data acquisition rates were achieved by scanning the target at speeds of 500 μ m/s and 1000 μ m/s using LCLS repetition rates of 5 Hz and 10 Hz, respectively. During each run, diffraction image data were recorded for each x-ray shot using the Cornell-SLAC Pixel Array Detector (CSPAD)¹⁹. Approximately 1/3 of the collected data contained measurable diffraction patterns. Data were analysed using Cheetah²⁰ and CrystFEL²¹ software suites.

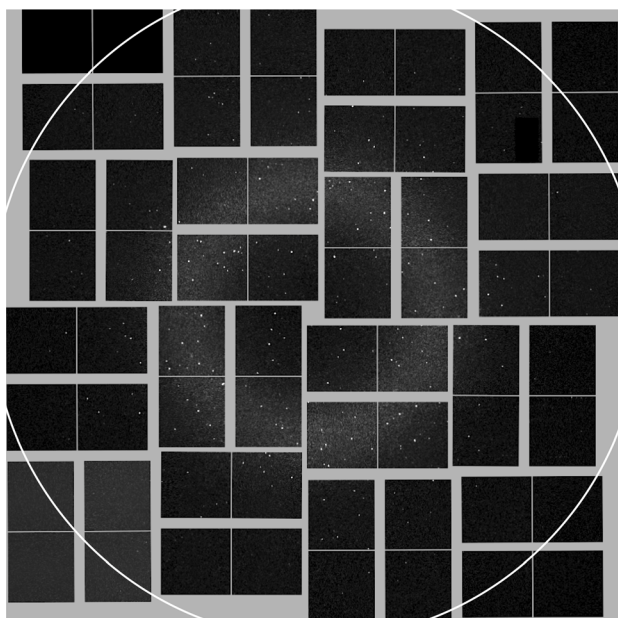


Figure 2 | Typical single diffraction pattern from a REP24 crystal preserved in Paratone-N using the CXI instrument of the LCLS. The diffraction pattern contains Bragg peaks to 2.5 Å resolution (2 Å resolution is indicated by the white circle) and was indexed with unit cell parameters that were consistent with the macrocrystal unit cell of REP24.

Diffraction patterns exhibited Bragg peaks to ~ 2.5 Å resolution (Fig. 2). Diffraction patterns were indexed with unit cell constants of $a = b = 44.44$ Å, $c = 183.45$ Å, $\alpha = \beta = 90^\circ$, and $\gamma = 120^\circ$, corresponding to a unit-cell volume of 313.8 nm³ and consistent with the unit cell constants of the macrocrystals of REP24 determined at a synchrotron pdb¹⁶ code 4P5P. The time between depositing the Paratone-N embedded crystals on the wafer and placing them into the vacuum of the CXI sample chamber to the time samples were measured by x-rays varied between 1–6 hours. There was no apparent degradation of diffraction quality over this time period. X-ray diffraction is an extremely sensitive measure of crystallinity and any degradation of crystal quality would rapidly lead to decreased resolution and spot sharpness, which supports that the crystals were protected from dehydration by the Paratone-N.

Six fast-scan data sets were collected from 10 μm crystals at high concentration (Table 1) with each run corresponding to one 200 μm × 8400 μm window. A total of 610 shots were taken, of which 233 were identified as having Bragg peaks from protein crystals, indicating a hit rate of 38.2%. The mean hit rate was calculated to be 38.2 (+/- 6.7)% for all of the runs. The total time taken to collect images from the 575 shots was 595 s (shot rate of $\sim 1/s$), however, the final three runs were completed in 99 s (for 90 shots each run)

approaching an average shot (and data acquisition) rate of 3/s and a hit rate of $\sim 1/s$.

Discussion

Two of the major challenges for FT-SFX at LCLS are the need to protect the protein crystals against dehydration as well as the current need to acquire $\sim 10^4$ diffraction patterns for a complete data set suitable for structure solution; previous fixed target experiments achieved data acquisition rates of 0.1 Hz or worse which is insufficient for FT-SFX.

Vacuum protection of protein microcrystals for FT-SFX experiments. Protecting protein crystals from dehydration in vacuum can be accomplished in one of two ways: 1) cryogenically cool the protein crystals, or 2) encapsulate the hydrated environment from the vacuum environment with a material that has minimal water permeability. We focused on encapsulating a hydrated environment so that room temperature data could be acquired, preserving the possibility of time resolved FT-SFX. To encapsulate a hydration environment, we embedded microcrystals in Paratone-N, an oil-based mixture with limited water permeability. Paratone-N is used in conventional protein crystallography as a cryo-protectant and was previously used for conventional structure determination of REP24 (pdb¹⁶ code 4P5P). REP24 macrocrystals embedded in Paratone-N for several days at room temperature remained visibly intact and maintained birefringence, indicating that there are no gross adverse effects of Paratone-N on REP24 crystals. Therefore, REP24 microcrystals embedded in Paratone-N were chosen as the first test sample for the FT-SFX experiments.

During initial development of the Paratone embedding procedure it was observed that at higher crystal densities, the protein crystals would cluster together and more thorough mixing was needed to increase the monodispersity of the crystal suspension. A potential solution for the clustering of the crystals would be to separate the crystals from the bulk aqueous phase in smaller batches, in a serial approach.

Data acquisition and hit rates for FT-SFX. Data were collected at a peak rate of 10 Hz and an average rate of 1/s, accounting for the time required to align the individual long membranes on the fixed target to the beam. The overall hit rate for diffraction patterns with Bragg peaks was 38%. This corresponds to ~ 0.3 hits/s at an average data acquisition rate of 1/s (average for all the runs discussed here) and ~ 1 hit/s at an average data acquisition rate of 3/s (average for the last three runs here). Assuming the “dead” time for aligning individual membranes can be significantly reduced by using optimized automated scripts for moving the sample stages and assuming LCLS operating at a shot rate of 10 Hz a hit rate of ~ 3 hits/s may be achievable and approach the ~ 5 hits/s rate previously demonstrated with lysozyme microcrystals using the liquid jet

Table 1 | The breakdown of the six runs for the fixed-target serial crystallography experiments using REP24. The three final runs were performed utilizing the 10-Hz scanning method for the data collection. The total time of 590 seconds was the amount of time it took for all six runs of data collection, including some movement and alignment of the windows before starting the fast scanning and the repositioning from one end of a long membrane to the beginning of the next long membrane. Therefore, the average shot and data acquisition rate during the six runs was $\sim 1/s$. It was 3/s for the last three runs

| Run number | Total shots | Total hits | Hit rate (%) | LCLS peak repetition rate (Hz) | Total time (s) |
|------------|-------------|------------|--------------|--------------------------------|----------------|
| 1 | 90 | 40 | 44.4 | 5 | |
| 2 | 125 | 50 | 40.0 | 5 | |
| 3 | 90 | 41 | 32.8 | 5 | |
| 4 | 90 | 31 | 34.4 | 10 | |
| 5 | 90 | 28 | 31.1 | 10 | |
| 6 | 90 | 43 | 47.8 | 10 | |
| Total | 575 | 233 | 38.2 | | 590 |



injector⁵. Such rates are significantly higher than typical data acquisition rates using fixed targets in other previous experiments at LCLS.

The peak data acquisition rate for FT-SFX will ultimately be determined by the linear velocity of the fixed target stage and the repetition rate of the LCLS due to a (putative) required minimum spacing between subsequent shots that will depend on the extent of the damage from the previous LCLS shot. The minimum useful spacing is dependent on the propagation of damage, but the extent to which damage caused by one LCLS pulse propagates through the sample to adjacent microcrystals is currently poorly characterized for FT-SFX, but the damage propagation will likely depend on the properties of the sample and embedding material. A minimum spacing of 100 μm was chosen for the experiments reported here to minimize effects of damage propagation, however, experiments at SACLA have indicated that damage propagation is contained within a 50 μm region from the sample²². For a given spacing between shots, the peak data acquisition rate will depend on the linear velocity of the motors. Using motors with higher linear velocities of several mm/s, FT-SFX data acquisition rates of 30 Hz or more may be possible.

For both FT-SFX and liquid jet (LJ)-SFX, crystal density is a key determinant of the achievable hit rate. For the liquid jet, the demonstrated hit rates for most samples have been ~ 1 –10%, far below the ideal hit rate of 63% for Poisson statistics ($\sim 63\%$ total hit rate, $\sim 37\%$ single crystal hits) that maximizes the single crystal hit rate. The hit rates achievable with the liquid jet are, in practice, often limited by clogging of the nozzle and/or a departure from ideal fluid behavior for suspensions with higher crystal densities. Fixed target approaches should allow for use of samples with higher crystal density²³ and therefore higher hit rates than allowed with the liquid jet because there is no requirement to maintain a stable jet. There are probably other practical limits on crystal density in FT-SFX because, for example, sample heterogeneity, or crystal clustering, may limit the achievable crystal density. Although a high crystal density leads to a higher hit rate, the concomitant clustering of the crystals could lead to an increase in patterns measured with multiple hits and a divergence from Poisson statistics for the single crystal hit rate. Multi-crystal hits may also prove useful as CrystFEL²¹ and other software packages such as cctbx.xfel²⁴ may be able to deconvolve and auto-index diffraction patterns from multiple lattices, provided the unit cell is known.

Time required for complete data sets in SFX. Our preliminary results showing vacuum protection of protein microcrystals and higher data acquisition rates with FT-SFX compared to previous fixed target work suggest FT-SFX is a potentially viable complementary method to the established LJ-SFX. To this end, it is useful to review the amount of sample and time required to produce complete data sets in recent LJ-SFX experiments compared to what will be achievable with FT-SFX.

The initial LJ-SFX experiments using Photosystem I³ involved 1.85×10^6 shots resulting in 8.5 \AA electron density maps reconstructed from 16374 patterns, although later analysis suggested as few as 10,000 patterns may be sufficient to achieve $\sim 100\%$ completeness¹⁵. Subsequent LJ-SFX experiments with lysozyme involved 1.5×10^6 shots, giving 66,432 patterns identified as “hits” of which 12,247 indexed patterns were used to calculate the electron-density map at 1.9 \AA resolution⁵. REP24 crystals have a high-symmetry space group ($P2_131$) and therefore a similar number of indexable patterns to that required for lysozyme should be sufficient to calculate an electron-density map of similar quality. Assuming a 10% indexing success rate and a 37% single hit rate, we can estimate that up to 340,000 shots would be needed for a complete data set (this may be an overestimate – only 140,000 shots would be needed if we assume a similar indexing success rate of $\sim 25\%$ as reported for lysozyme ref. 5). At 1 Hz average data collection rate, this would require

95 hours of data collection and 125 fixed target wafers similar to the ones used here (Supplementary Fig. 1). To collect data from 1.5×10^6 shots⁵ at 120 Hz with the liquid jet would require a minimum of 3.5 hours of continuous operation. However, if the average data collection rate for the fixed-target experiments can be increased to 10/s (as compared to the 1–3/s data collection rate demonstrated in the present work), the total collection time can be reduced to less than 10 hours, which is less than one shift of LCLS beam time.

Sample consumption for SFX. Although LJ-SFX currently has a clear advantage over FT-SFX with regard to data acquisition rate, FT-SFX has the potential to drastically reduce sample consumption compared to the current LJ-SFX method. We calculate that FT-SFX could save several orders of magnitude in sample consumption, compared to the LJ-SFX (details provided in supplemental information). The LJ-SFX method with the current liquid jet injector requires a minimum of several tens of milligrams of protein to collect a complete data set^{3,5}. For an optimized FT-SFX experiment using 700 nm protein crystals with the 1.3 μm LCLS focus, we calculate that we would need $\sim 230 \mu\text{g}$ of protein to collect a complete data set, which would reduce the sample demand by at least two orders of magnitude and will be useful for low-abundance proteins, or proteins that are expensive to produce in milligram quantities, such as recombinantly expressed membrane proteins. (It should be noted, that in the cases where the above mentioned electrospinning jet or LCP jet can be used this sample requirement can be pushed also to below 1 mg).

Areas of improvement for FT-SFX. A persistent challenge for FT-SFX will be protecting protein crystals from the vacuum of XFEL sample chambers. Paratone-N embedding was shown to work for crystals of REP24 (and a few other soluble proteins, such as lysozyme), but is not a generally applicable vacuum protectant; membrane protein crystals dissolve in Paratone-N, for example. Mounting crystals in sealed macro hydration cells, in which the protein crystals remain in their mother liquor, could prove a more generalizable method for FT-SFX. Such a hydration cell configuration would need to be compatible with high data acquisition rates, however. Future work with FT-SFX will clearly require further development of methods to encapsulate hydration environments for microcrystals. XFEL sample chambers may also be equipped with cryo-stages, but that would detract from two of the clear utilities of XFELs for structural biology, namely ultrafast time resolved studies and the study of structures at room temperature.

Another potential issue may be preferential alignment of crystals (e.g., long, needle-like crystals preferentially laying flat on the substrate surface) that might not allow a full sampling of reciprocal space for a substrate surface perpendicular to the incident X-rays, which would impact structure determination. However, this issue, if encountered, can be easily mitigated by the use of a goniometer stage to rotate the normal vector of the fixed target support relative to the incident X-rays. Such a goniometer stage is already available at LCLS and has been used by the authors in other experiments.

It is clear, that for FT-SFX to be viable, an increase in the peak and average shot rates is required. The most straightforward way of achieving the required spacing between shots at high shot rates will be to have motors with faster translational motion for the fixed target stage, which will allow for higher repetition rates while maintaining the necessary minimum separation between shots, and optimized automated scripts that move the fixed target from the end of one long membrane to the beginning of the next long membrane with minimal dead time for data acquisition. Another method to increase the average data acquisition rate would be to use windowless sample supports. Windowless supports would increase the number of LCLS shots per given area of the sample holder (the shot density) because there are no supports to impede the transmission of the x rays, and windowless supports would make overall alignment time negligible.



Outlook. Both liquid jet injection and the fixed target approach have their advantages and disadvantages and thus are complementary techniques. LJ-SFX techniques offer the advantage of fully hydrated samples (microcrystals can be injected in the mother liquor) and are compatible with future XFEL sources that will have much higher repetition rate (e.g. the EXFEL with ~ 30 kHz repetition rate²⁵). In contrast, in FT-SFX, microcrystal samples will need to be protected from dehydration (e.g. by embedding in oil or enclosing in hydration chambers) and the data acquisition rate may always be somewhat limited in practice (probably to a few tens per second) by motor speeds, minimum spacing between shots and required mechanical precision. On the other hand, at present, FT-SFX seems to offer a straightforward path to reducing sample consumption for the lower repetition rate XFEL sources, such as LCLS. Moreover, FT-SFX may offer advantages for certain types of time-resolved studies compared to the liquid jet, in particular, optical pump/x-ray probe experiments that involve relatively long pump-probe delay times and/or multiple optical excitation pulses as well as other types of pump-probe experiments that involve e.g., electric field pulses or chemical reactions triggered by liquid mixing by microfluidics.

- Arthur, J. *et al.* The LCLS – A 4th-generation light-source using the SLAC Linac. *Rev. Sci. Instrum.* **66**, 1987–1989 (1995).
- Emma, P. *et al.* First lasing and operation of an Ångström-wavelength free-electron laser. *Nat. Photonics* **4**, 641–647 (2010).
- H, N. Chapman, H. N. *et al.* Serial femtosecond nanocrystallography. *Nature* **470**, 73–81 (2011).
- Hunter, M. S. *et al.* X-ray Diffraction from Membrane Protein Nanocrystals. *Biophys. J.* **100**, 198–206 (2011).
- Boutet, S. *et al.* High-Resolution Protein Structure Determination by Serial Femtosecond Crystallography. *Science* **337**, 362–364 (2012).
- Redecke, L. *et al.* Natively Inhibited *Trypanosoma brucei* Cathepsin B Structure Determined by Using an X-ray Laser. *Science* **339**, 227–230 (2012).
- Liu, W. *et al.* Serial Femtosecond Crystallography of G Protein-Coupled Receptors. *Science* **342**, 1521–1524 (2013).
- Spence, J. C. H., Weierstall, U. & Chapman, H. N. X-ray lasers for structural and dynamic biology. *Rep. Prog. Phys.* **75**, 1–25 (2012).
- Weierstall, U. *et al.* Droplet streams for serial crystallography of proteins. *Exp. Fluids* **44**, 675–689 (2008).
- DePonte, D. P. *et al.* Gas dynamic virtual nozzle for generation of microscopic droplet streams. *J. Phys. D: Appl. Phys.* **41**, 195505 (2008).
- Weierstall, U., Spence, J. C. H. & Doak, R. B. Injector for scattering measurements on fully solvated biospecies. *Rev. Sci. Instrum.* **83**, 1–12 (2012).
- Sierra, R. G. *et al.* Nanoflow electrospinning serial femtosecond crystallography. *Acta Crystallogr. D.* **68**, 1584–1587 (2012).
- Weierstall, U. *et al.* Lipidic cubic phase injector facilitates membrane protein serial femtosecond crystallography. *Nat. Commun.* **5**, 1–6 (2014).
- Kirian, R. A. *et al.* Femtosecond protein nanocrystallography-data analysis methods. *Opt. Express* **18**, 5713–5723 (2010).
- Kirian, R. A. *et al.* Structure-factor analysis of femtosecond micro-diffraction patterns from protein nanocrystals. *Acta Crystallogr. A* **67**, 131–140 (2011).
- Berman, H. M. *et al.* The Protein Data Bank. *Nucl. Acids Res.* **28**, 235–242 (2000).
- Boutet, S. & Williams, G. J. The Coherent X-ray Imaging (CXI) instrument at the Linac Coherent Light Source (LCLS). *New J. Phys.* **12**, 035024 (2010).
- Boutet, S. personal communications discussing completed experiments at CXI using XTCAV diagnostics (2014).
- Hart, P. *et al.* The CSPAD megapixel x-ray camera at LCLS. *Proc. SPIE* **8504**, 85040C (2012).
- Barty, A. *et al.* Cheetah: software for high-throughput reduction and analysis of serial femtosecond X-ray diffraction data. *J. Appl. Crystallogr.* **47**, 1118–1131 (2014).
- White, T. A. *et al.* CrystFEL: A software suite for snapshot serial crystallography. *J. Appl. Crystallogr.* **45**, 335 (2012).
- Hirata, K. *et al.* Determination of damage-free crystal structure of an X-ray-sensitive protein using an XFEL. *Nat. Methods* doi:10.1038/nmeth.2962 (2014)
- Park, J. *et al.* Monte Carlo study for optimal conditions in single-shot imaging with femtosecond x-ray laser pulses. *Appl. Phys. Lett.* **103**, 264101 (2013).
- Sauter, N. K. *et al.* New Python-based methods for data processing. *Acta Crystallogr. D* **69**, 1274–1282 (2013).
- Geloni, G. *et al.* Coherence properties of the European XFEL. *New J. Phys.* **12**, 035021 (2010).

Acknowledgments

Work was performed under the auspices of the U.S. Department of Energy by Lawrence Livermore National Laboratory under contract DE-AC52-07NA27344 and Pacific Northwest National Laboratory (operated by Battelle Memorial Institute) under Contract DE-AC05-76RL01830 and carried out at the Linac Coherent Light Source (LCLS) at SLAC National Accelerator Laboratory. LCLS is an Office of Science User Facility operated for the U.S. Department of Energy Office of Science by Stanford University. Support was provided by the UCOP Lab Fee Program (award no 118036), the LLNL Laboratory Directed Research and Development (LDRD) program under project 12-ERD-031, and the National Science Foundation under project MCB 1021577. We would like to thank G. M. Stewart and SLAC Infomedia for generating Fig. 1.

Author contributions

MSH, BWS, SPH-R, MC, WHB, JE, and MF conceived the experiment. MSH, BWS, SB, and MF designed the experiment. MSH and BSW prepared the REP24 and applied it to the fixed-target supports. MM, MSH, BWS, DBC, AB, MC, WHB, AG, SPH-R, TP, GJW, SB, MMS, NAZ, and MF collected the data. MM, MMS, GJW, and SB installed the motors and designed and installed other hardware and software used for the experiments. NAZ and MSH processed and interpreted the data. All authors reviewed the manuscript.

Additional information

Supplementary information accompanies this paper at <http://www.nature.com/scientificreports>

Competing financial interests: The authors declare no competing financial interests.

How to cite this article: Hunter, M.S. *et al.* Fixed-target protein serial microcrystallography with an x-ray free electron laser. *Sci. Rep.* **4**, 6026; DOI:10.1038/srep06026 (2014).



This work is licensed under a Creative Commons Attribution-NonCommercial-NoDerivs 4.0 International License. The images or other third party material in this article are included in the article's Creative Commons license, unless indicated otherwise in the credit line; if the material is not included under the Creative Commons license, users will need to obtain permission from the license holder in order to reproduce the material. To view a copy of this license, visit <http://creativecommons.org/licenses/by-nc-nd/4.0/>